# Multi-scale Wasserstein Shortest-path Filtration Kernels on Graphs

Wei Ye, Hao Tian, and Qijun Chen, Senior Member, IEEE

Abstract—The traditional shortest-path graph kernel (SP) is one of the most popular graph kernels, which decomposes graphs into shortest paths and counts their frequencies in each graph. However, SP has two main challenges: Firstly, the triplet representation of the shortest path loses information. Secondly, SP compares graphs without considering the multiple different scales of the graph structure which is common in real-world graphs, e.g., the chain-, ring-, and star-structures in social networks. To mitigate these two challenges, we develop a novel shortest-path graph kernel called the Multi-scale Wasserstein Shortest-Path Filtration graph kernel (MWSPF). It uses a BFS tree of a certain depth rooted at each vertex to restrict the maximum length of the shortest path considering the small world property. It considers the labels of all the vertices in the shortest path. In order to compare graphs at multiple different scales, it augments graphs from both the aspects of the vertex and the graph structure. The distribution (frequency) of the shortest path changes across augmented graphs and the Wasserstein distance is employed to track the changes. We conduct experiments on various benchmark graph datasets to evaluate MWSPF's performance. MWSPF is superior to the state-of-the-art on most

Index Terms—graph kernels, shortest path, graph filtration, multiple different scales, Wasserstein distance

#### I. INTRODUCTION

Graph-structured data is prevalent in many domains such as social networks, transportation networks, and molecules. One fundamental problem for graph-structured data is to compute their similarities, which can facilitate downstream tasks such as graph classification. Graph kernels are conventional methods for this purpose. Most graph kernels are instances of the R-convolution kernels [1] that decompose graphs into substructures and aggregate the substructure similarity as graph similarity without considering the distribution of the substructures. Substructures used in graph kernels can be walks [2]–[4], paths [5], [6], subgraphs [7]–[10], and subtree patterns [11]–[16].

In the real world, many graphs have the small world property [17]. For a vertex, most of its neighboring vertices can be reached from every other vertex by a small number of hops. In other words, the mean shortest-path length is small. Thus, the shortest-path graph kernel (SP) [5] is a natural method to compute similarities between such kinds of graphs. We study SP in this paper. In graph theory [18], the shortest path between two vertices in a graph is defined as a path that connects these two vertices with the minimum sum of the

Manuscript received xxx; revised xxx.

The authors are with the College of Electronic and Information Engineering, Tongji University, Shanghai 201804 China (e-mail: {yew, 2133036, qjchen}@tongji.edu.cn).

weights of its constituent edges. The substructure used in SP is the shortest path. SP represents the shortest path between each pair of vertices by a triplet whose elements are the labels of source and sink vertices and the length of this shortest path. The representation of the shortest path in SP treats all edges equally, i.e., each edge has a weight value of one. Each graph is represented as a bag of triplets. SP counts the frequencies of each triplet in each graph. However, using such a triplet to represent the shortest path is very coarse and may lose information. For example, two shortest paths having the same source and sink vertex labels and the same length will be represented as the same triplet, no matter what other vertices they have passed by.

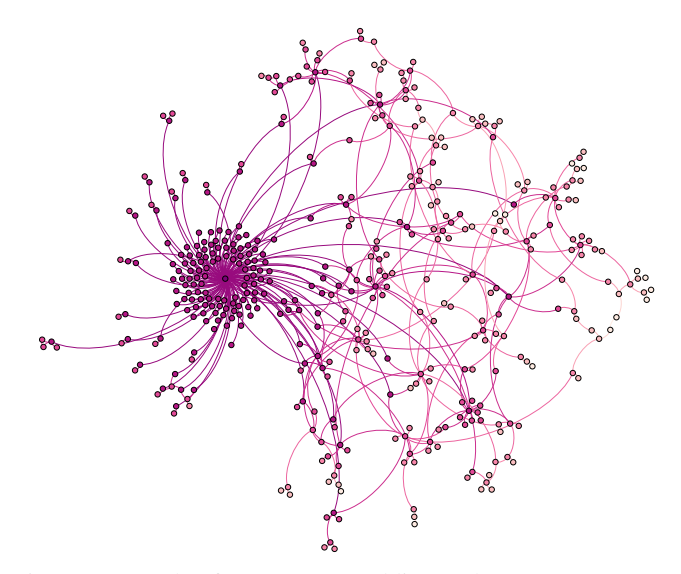


Fig. 1: A graph of a post on Reddit. Each vertex represents a user. Two users are connected by an edge if at least one of them responds to the other's comment. The image is drawn with Gephi.

In the real world, many graphs, such as social networks, also have multiple different scales of the graph structure. Figure 1 shows an online discussion thread on Reddit<sup>1</sup>. Users are represented as vertices. If a user responds to another user's comment, these two users are connected by an edge. It is evident that this graph contains multiple different scales of the graph structures, such as chain, ring, and star. If a graph kernel can not only differentiate the overall shape of graphs but also their small substructures, it will be more versatile. Although SP has a competitive performance to some advanced

<sup>1</sup>https://www.reddit.com/r/AskReddit

multi-scale graph kernels such as MLG (Multi-scale Laplacian Graph kernel) [10], it cannot compare graphs at multiple different scales, because shortest paths cannot directly reveal the full neighborhood structure (i.e., one-hop neighbors, two-hop neighbors ···) around a vertex compared with the subtree pattern used in the WL graph kernel [14].

To overcome the two challenges pertinent to SP, in this paper, we propose a novel multi-scale Wasserstein shortestpath filtration graph kernel (MWSPF). Instead of computing all the shortest paths between each pair of vertices, we construct a BFS tree of depth d rooted at each vertex and only consider the shortest paths from the root to any other vertices in this BFS tree as graph features. d is a parameter that controls the maximum length of the shortest paths. Our motivation comes from two perspectives: 1) A path from the root of a BFS tree to any other vertices in this BFS tree is a shortest path. Combining SP with the BFS tree is natural; 2) the small world property. To consider more finer information in the shortest path, we do not use the triplet representation as used in SP. We not only consider the labels of the source and sink vertices but also the labels of the intermediate vertices along the shortest path. To this end, we represent the shortest path as the concatenation of all the labels of vertices in this shortest path. Compared with the triplet representation, our new representation can compare graphs at a finer granularity. To render SP capable of comparing graphs at multiple different scales, we propose two strategies to augment graphs: 1) extracting different scales of structural or topological information (represented by the BFS trees of different depth k) around vertices to augment vertex; 2) generating graph filtration that is a sequence of nested subgraphs that differ only in the sets of edges to augment the graph structure. Note that graph filtration can also make SP capable of comparing graphs with continuous edge or vertex attributes. Finally, each graph is represented by a set of vectors which are called shortest-path graph feature maps, each element of which represents the frequencies of shortest paths in an augmented graph. We adopt the Wasserstein distance to compute the distance between two sets of graph feature maps, considering the distribution (frequency) of shortest paths across augmented graphs. The Wasserstein distance is transformed into graph similarity by the Laplacian RBF kernel.

Our main contributions can be summarized as follows:

- We represent each shortest path as the concatenation of all its vertex labels rather than the simple triplet. This representation takes into account all the vertex label information in the shortest path and can compare graphs at local scales.
- We extract different scales of structural or topological neighborhood information around a vertex by constructing BFS trees of different depths. Each BFS tree is hashed into a unique integer label that is used to augment vertex, aggregating different scales of neighborhood information.
- We generate graph filtration to augment the graph structure. The frequency of each shortest path changes across graph filtration. We use the Wasserstein distance to track the changes.
- We show in the experiments that our graph kernel

MWSPF outperforms state-of-the-art graph kernels on most benchmark datasets.

The rest of the paper is organized as follows: We discuss related work in the following section. Section 3 describes the preliminaries. Section 4 introduces our method, including the shortest-path graph feature map, vertex augmentation, graph structure augmentation, and our graph kernel MWSPF. Section 5 compares MWSPF with state-of-the-art graph kernels for the task of graph classification on the benchmark datasets. Section 6 concludes the paper.

#### II. RELATED WORK

Graph kernels are traditional methods for graph classification. Most graph kernels belong to the family of Rconvolution kernels [1] that decompose graphs into substructures and aggregate these substructure similarities as final graph similarity. Random walk graph kernels [2], [3] count the number of matching random walks on two graphs. This can be conducted by performing random walks on the direct product graph of two graphs. Random walk graph kernels can be closed-form [2] with the help of the personalized PageRank diffusion [19] and the heat kernel diffusion [20]. RetGK [4] generates for each vertex a feature vector, whose elements represent the return probability of a random walk starting from and ending in the same vertex with different numbers of hops. This feature vector is combined with vertex discrete or continuous features and Maximum Mean Discrepancy (MMD) [21] is adopted to compute graph similarity. SP [5] counts the frequencies of two shortest paths, which have the same triplet representation (the same source and sink labels and the same length) in two graphs. NSPDK [8] decomposes a graph into all pairs of neighborhood subgraphs of different radium. MLG [10] can compare graphs at multiple different scales, which are represented by a hierarchy of nested subgraphs with varying scales. WL [13], [14] is based on the Weisfeiler-Lehman test of graph isomorphism [22]. The substructure used in WL is the subtree pattern. WWL [16] is an extension of WL. It is able to compare graphs with continuous vertex attributes. It represents each graph as a set of vertex embeddings and uses the one-dimensional Wasserstein distance to compute graph similarity. Each vertex is associated with two kinds of features, one of which is the embedding generated by the WL and the other of which is continuous attributes. The continuous attributes of each vertex are averaged with those of its neighboring vertices by an average aggregation operator, which is inspired by the message-passing mechanism of Graph Convolutional Networks (GCN) [23].

DGK [24] adopts word2vec [25] to learn representations for graph substructures. The similarity between graph substructures is computed and integrated into the final graph kernel matrix. OA [26] first generates graph hierarchies and then computes the optimal assignment kernels, which are integrated into the WL. PM [27] uses the eigenvectors of the graph adjacency matrices as graph embeddings and uses the Pyramid Match kernel [28], [29] to compute graph similarity. HTAK [30] transitively aligns the vertices between graphs through a family of hierarchical prototype graphs, which are

generated by the K-means clustering method. FWL [31] is a combination of graph filtrations and WL. Compared with WL, FWL's expressiveness is more powerful. There are some connections between over-parameterized neural networks and kernel methods [33], [34]. GNTK [32] is developed considering such connections. It has both the advantages of graph neural networks (GNNs) and graph kernels and equals to infinitely wide GNNs trained by gradient descent.

The graph kernels described above cannot classify graphs with continuous vertex attributes. GraphONTK [35] introduces the attention mechanism into GNTK and accelerates GNTK by quantum computing. CSM [36] is a graph kernel for attributed graphs, which is based on subgraph matchings and allows to rate mappings of subgraphs by a flexible scoring scheme. GH [37] extends the shortest-path graph kernel. GH compares shortest paths using kernels on the vertices of shortest paths. ODD [38] maps each graph into a multiset of decomposition Directed Acyclic Graph (DAG), which is encoded as a unique string for ordering. The ordered DAG is mapped into a multiset of trees. ODD introduces a kernel on continuous vertex attributes wherever the discrete labels of two vertices match. HGK [39] iteratively maps continuous attributes to discrete labels by randomized hash functions. Then, WL or SP is used to compare these discretized graphs. GIK [40] uses a vertex invariant kernel (called spectral coloring kernel) to compute both the similarities of vertex labels and vertex structural roles. IGK [41] first uses isolation kernel [42] on the vertex attribute vectors to generate vertex embeddings, which are then propagated into the graph structure by the average aggregation operator in WWL. Finally, kernel mean embedding [43] is applied on all the vertex embeddings to generate graph embedding which is used to compute graph kernels.

## III. MULTI-SCALE WASSERSTEIN SHORTEST-PATH FILTRATION GRAPH KERNELS

In this section, let us first give notations used in this paper and then describe the details of our multi-scale Wasserstein shortest-path filtration graph kernels (MWSPF).

### A. Notations

In this work, boldface lowercase letters (e.g., x = $[x_1,\ldots,x_n]$ ) represent row vectors. Similarly, boldface uppercase letters  $\mathbf{X} = [\mathbf{x}_1; \dots; \mathbf{x}_n]$  represent matrices. An (undirected and unweighted) graph is represented by  $\mathcal{G} = (\mathcal{V}, \mathcal{E})$ , where V represents vertices and E represents graph edges. An edge e is denoted by two vertices (v, v') that are connected to it.  $\mathcal{N}(v)$  denotes the neighboring vertices of vertex  $v \in \mathcal{V}$ , i.e.,  $\mathcal{N}(v) = \{v' \in \mathcal{V} | (v, v') \in \mathcal{E}\}. \mid \cdot \mid \text{ denotes the size of a }$ set. An attributed graph is a graph  $\mathcal{G}$  with an attribute function  $a: \mathcal{V} \to \mathbb{R}^m (m \geq 1)$ . A labeled graph is a graph  $\mathcal{G}$  with a label function  $l: \mathcal{V} \to \Sigma$ , where  $\Sigma$  is a finite label alphabet. Without loss of generality,  $|\Sigma| \leq |\mathcal{V}|$ . A graph can have both continuous vertex attributes and categorical vertex labels. a(v)denotes the attribute of v (i.e., the high-dimensional continuous vectors), and l(v) denotes the categorical label of v (i.e., integer numbers encoding either an ordered discrete value or a category). The depth of a BFS tree is the maximum length of the shortest path between the root and any other vertex in this BFS tree.

Let  $\mathcal{X}$  be a non-empty set and  $\kappa: \mathcal{X} \times \mathcal{X} \to \mathbb{R}$  be a function on  $\mathcal{X}$  associated with a Hilbert space  $\mathcal{H}$ , such that there exists a feature map  $\phi: \mathcal{X} \to \mathcal{H}$  with  $\kappa(x,y) = \langle \phi(x), \phi(y) \rangle$  for all x, y in  $\mathcal{X}$ , where  $\langle \cdot, \cdot \rangle$  denotes the inner product of  $\mathcal{H}$ . Then,  $\mathcal{H}$  is a reproducing kernel Hilbert space (RKHS) and  $\kappa$ is a symmetric and positive-semidefinite kernel, which can be used by support vector machines (SVM) for classification. For graphs, let  $\phi(\mathcal{G})$  denote a mapping from a graph to a vector, whose entry represents the frequencies of the substructures (such as the shortest path) in graph  $\mathcal{G}$ . Then, the kernel on two graphs  $\mathcal{G}$  and  $\mathcal{G}'$  is defined as  $\kappa(\mathcal{G}, \mathcal{G}') = \langle \phi(\mathcal{G}), \phi(\mathcal{G}') \rangle$ , which denotes the sum of substructure similarities and is the basis of the R-convolution graph kernels. However, the R-convolution graph kernels using the aggregation of substructure similarities neglect valuable information, such as substructure distribution. Thus, in this paper we use the Wasserstein distance to better compute the graph similarity, considering the distribution of the substructures across augmented graphs.

#### B. Augment Vertex

Formally, graph feature maps are defined as follows:

**Definition 1** (Graph Feature Maps). Given an undirected and unweighted graph  $\mathcal{G}$  that has a set of non-isomorphic substructures  $\{A_1, A_2, \ldots, A_r\}$ , define a map  $\psi : \mathcal{G} \times \Sigma \to \mathbb{N}$  such that  $\psi(\mathcal{G}, A_i)(1 \leq i \leq r)$  is the frequencies of the substructure  $A_i$  in graph  $\mathcal{G}$ . The graph feature map of  $\mathcal{G}$  is defined as follows:

$$\phi(\mathcal{G}) = [\psi(\mathcal{G}, \mathcal{A}_1), \psi(\mathcal{G}, \mathcal{A}_2), \dots, \psi(\mathcal{G}, \mathcal{A}_r)]$$
 (1)

where r is the number of non-isomorphic substructures in graphs.

For each shortest path  $\mathcal{P}="s,v_1,v_2,\ldots,t"\in\mathcal{G}$  where s and t denote the source and target vertex, respectively. The shortest-path graph kernel (SP) [5] represents shortest path  $\mathcal{P}$  as a triplet  $T=(l(s),l(t),len(\mathcal{P}))$ , where  $len(\mathcal{P})$  is its length. For instance, in Figure 2(a), the triplet representation of the shortest path starting from the leftmost vertex and ending in the rightmost vertex is (2,1,4). Then, for graph  $\mathcal{G}$ , its feature map is computed as follows:

$$\phi(\mathcal{G}) = [\psi(\mathcal{G}, T_1), \psi(\mathcal{G}, T_2), \dots, \psi(\mathcal{G}, T_r)]$$
 (2)

We can see from the above that the triplet representation of the shortest path only contains the labels of the source and target vertices. The labels of other vertices in the shortest path between the source and target vertices are not considered. Two shortest paths, starting from the same source vertex and ending in the same target vertex and having the same length, will be represented as the same triplet and treated equally. However, the labels of other vertices except the source and target vertices in these two shortest paths may differ a lot. Without considering this aspect in the representation of shortest paths, finer information cannot be included in the representation.

To mitigate this problem of SP, we take into account the labels of all the vertices in the shortest path. Let us give the definition of shortest-path representation used in this paper as follows:

**Definition 2** (Shortest-path Representation). Given an undirected, unweighted, and labeled graph  $\mathcal{G} = (\mathcal{V}, \mathcal{E}, l)$ , a BFS tree  $\mathcal{T} = (\mathcal{V}', \mathcal{E}', l)$  ( $\mathcal{V}' \subseteq \mathcal{V}$  and  $\mathcal{E}' \subseteq \mathcal{E}$ ) of depth d rooted at each vertex  $v \in \mathcal{V}$  is constructed. v is the root of  $\mathcal{T}$ . For each vertex  $v' \in \mathcal{V}'$ , the shortest path is constructed by concatenating all the distinct vertices and edges from the root v to v', i.e.,  $\mathcal{P} = \text{``}v, v_1, v_2, \dots, v'$ ''. The shortest-path representation is the concatenated labels of all the vertices in this shortest path, i.e.,  $\text{``}l(v), l(v_1), l(v_2), \dots, l(v')$ ''.

Figure 2(b) shows a BFS tree  $\mathcal{T}_1$  of depth d=1 rooted at the left-bottom vertex with label 1 in  $\mathcal{G}$ . All the shortest paths starting from the root are "1", "1, 3", "1, 3". Note that we also consider the shortest path of length zero, whose source and target vertices are itself.

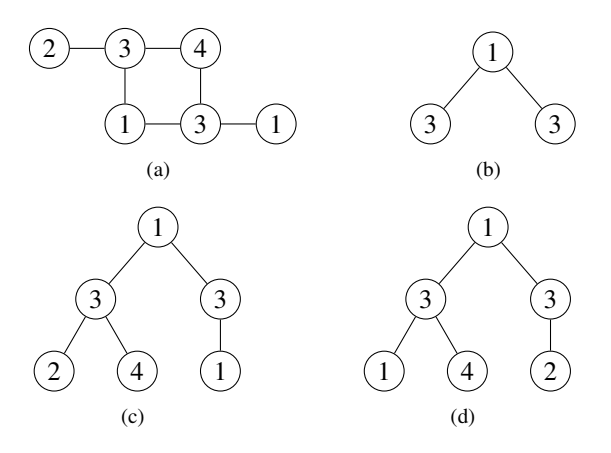


Fig. 2: (a) An undirected labeled graph  $\mathcal{G}$ .  $\Sigma = \{1, 2, 3, 4\}$ . (b) A BFS tree of depth one rooted at the left-bottom vertex with label 1 in graph  $\mathcal{G}$ . (c) A BFS tree of depth two rooted at the left-bottom vertex with label 1 in graph  $\mathcal{G}$ . (d) Another BFS tree of depth two rooted at the left-bottom vertex with label 1 in graph  $\mathcal{G}$ .

In addition to the aforementioned problem, SP cannot compare graphs at multiple different scales, because paths cannot directly reveal the structural neighborhood information of vertices. Thus, we need to augment the vertex by extracting the different scales of the graph structure around it and integrating the multi-scale information into the representation of shortest paths. In this work, we augment the vertex by hashing a BFS tree of depth k (capturing different scales of the graph structure around a vertex) rooted at this vertex to an integer label, aggregating the neighborhood structural information. Since the construction of a BFS tree rooted at a vertex may be not unique, we propose a method to construct a BFS tree that has a unique representation.

We construct a BFS tree of depth k rooted at a vertex layer by layer. In each layer, we sort vertices in ascending order with regard to their label values. If the label values of two vertices are the same, we sort these two vertices according to the

representations of the BFS trees of depth one rooted at them. We use Figure 2 as an example to explain our method. To construct a BFS tree of depth k=2 rooted at the left-bottom vertex with label 1 in Figure 2(a), we first construct a BFS tree of depth one as shown in Figure 2(b), which is represented by the concatenation of all its edges, i.e., "1, 3, 1, 3". For each child vertex in Figure 2(b), we constructuild a BFS tree of depth one rooted at it. The two child vertices in Figure 2(b) have the same label values that will lead to the uncertainness in the vertex order, which will generate uncertain BFS trees as shown in Figure 2(c) and (d), respectively. In order to generate certain BFS trees, we consider the neighborhood structural information of these two child vertices, i.e., comparing the representations of the BFS trees of depth one rooted at them. The representations of the BFS trees of depth one rooted at them are "3, 2, 3, 4" and "3, 1, 3, 4", respectively. Thus, we adopt the BFS tree of depth two shown in Figure 2(d) as the final BFS tree. Note that if these two BFS trees of depth one have the same representation, we will recursively construct BFS trees of depth one rooted at the descendants of these two child vertices until they can be distinguished or reach the maximum depth k = K. Finally, the BFS tree shown in Figure 2(d) can be represented as "1, 3, 1, 3 - 3, 1, 3, 4 - 3, 2", which is the concatenation of the representations of all the BFS trees of depth one in it.

Note that we use the dash symbol "-" to concatenate the representations of different BFS trees of depth one in order to make the representation of the BFS tree of depth k injective. For example, Figure 3 shows two BFS trees of depth two. Without using the dash symbol "-", the representation of them is the same, i.e., "1,3,1,3,3,1,3,1,3,2". But with the help of the dash symbol, the representation of the left BFS tree is "1,3,1,3-3,1,3,1-3,2" and that of the right BFS tree is "1,3,1,3-3,1-3,1,3,2". Their representations are distinguishable.

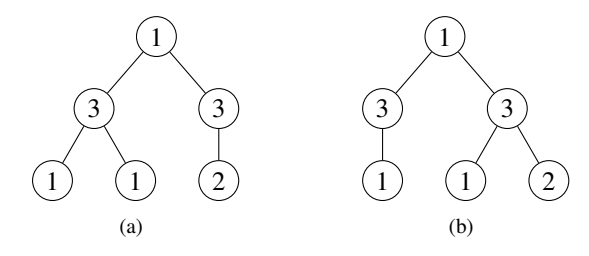


Fig. 3: Two example BFS trees of depth two.

All BFS trees of depth k rooted at each vertex in a graph are constructed and represented by strings using the above method. All the unique strings are sorted lexicographically and kept in a set. We can use the index of each BFS tree (its string representation) in the set as its label. Figure 4(a) and (c) show the two augmented graphs  $\mathcal{G}^{(1)}$  and  $\mathcal{G}^{(2)}$  of graph  $\mathcal{G}$ , when k is set to 1 and 2 respectively. We can see that the two vertices with the same label 3 in  $\mathcal{G}$  have different new labels in  $\mathcal{G}^{(1)}$  and  $\mathcal{G}^{(2)}$  because these two vertices have the different structural neighborhood. By constructing BFS trees of different depths k, we can capture different scales of the graph structure around a vertex. For each vertex in each augmented graph, we construct

5

a BFS tree of depth d rooted at this vertex and count all the shortest paths which will be used for computing the shortest-path graph feature map. For example, Figure 4(b) shows a BFS tree of depth one rooted at the vertex with label 6 in Figure 4(a). All the shortest paths starting from the root are "6", "6,8", "6,9". Note that if k=0 the augmented graph is just the original graph.

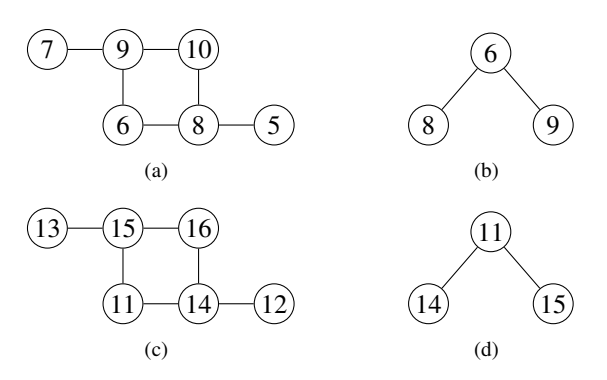


Fig. 4: (a) The augmented graph  $\mathcal{G}^{(1)}$ , when k=1.  $\Sigma=\{5,6,7,8,9,10\}$ ; (b) A BFS tree of depth one rooted at the vertex with label 6 in  $\mathcal{G}^{(1)}$ ; (c) The augmented graph  $\mathcal{G}^{(2)}$ , when k=2.  $\Sigma=\{11,12,13,14,15,16\}$ ; (d) A BFS tree of depth one rooted at the vertex with label 11 in  $\mathcal{G}^{(2)}$ .

In this paper, to make our graph kernel multi-scale, we concatenate all the shortest-path graph feature maps extracted from  $\mathcal{G}^{(0)}, \mathcal{G}^{(1)}, \dots, \mathcal{G}^{(k)}$  as follows:

$$\phi(\mathcal{G}) = \parallel_{i=0}^{k} \phi(\mathcal{G}^{(i)}) \tag{3}$$

#### C. Augment the Graph Structure

In the last section, by hashing the BFS tree of depth krooted at each vertex to an integer label (i.e., aggregation of neighborhood information), the graph vertex is augmented, which makes SP aware of the multi-scale structural or topological information around vertices. In addition to augmenting the vertex, we augment the graph structure in this section to generate multiple different scales of the graph structure. We use the concept of filtrations [45], [46] to generate a sequence of nested subgraphs that differ only in the sets of edges based on the edge weights. Such a sequence can be considered as constructing a graph by gradually adding sets of edges whose weights satisfy some criterion. This can also be viewed as incremental graph structure augmentation. In addition to generating multiple different scales of the graph structure, graph filtration can make SP capable of comparing graphs with continuous edge or vertex attributes. Note that in this paper edge weights are only used for generating graph filtrations. The construction of the shortest path does not consider edge weight.

The graph flitration is defined as follows:

**Definition 3** (Graph Filtration). Given an undirected and unweighted graph  $\mathcal{G} = (\mathcal{V}, \mathcal{E})$ , we use a weight function  $\mathbf{w} : \mathcal{E} \to \mathbb{R}$  to assign weights to its edges. All unique edge weight values are sorted in ascending order, i.e.,  $w_1 \leq w_2 \leq$ 

 $\cdots \leq w_q$ . Then, the graph filtration of  $\mathcal{G}$  is defined as a sequence of nested subgraphs:

$$\mathcal{G}_1 \subseteq \mathcal{G}_2 \subseteq \ldots \subseteq \mathcal{G}_q = \mathcal{G} \tag{4}$$

where  $G_i = (V_i, \mathcal{E}_i)(1 \le i \le q)$ , with  $V_i \subseteq V$  and  $\mathcal{E}_i = \{e \in \mathcal{E} | \mathbf{w}(e) \le w_i\} \subseteq \mathcal{E}$ .

The above definition also works for weighted graphs whose edges have inherent weights. But in this paper, we only focus on unweighted graphs, for which we can use different kinds of weight functions to generate edge weights and graph filtrations. For unweighted graphs with continuous vertex attributes, the edge weight between vertices  $v_i$  and  $v_j$  is set as the Euclidean distance between their attributes:  $w_{ij} = \|a(v_i) - a(v_j)\|_2$ . For unweighted graphs with categorical vertex labels, the edge weight between vertices  $v_i$  and  $v_j$  is set as the Jaccard distance between them. The Jaccard distance is calculated as follows:

$$d(v_i, v_j) = 1 - \frac{|\mathcal{N}(v_i) \cap \mathcal{N}(v_j)|}{|\mathcal{N}(v_i) \cup \mathcal{N}(v_j)|}$$
(5)

where  $|\cdot|$  represents the size of a set.

Figure 5 shows an example of graph filtration and we denote the filtration of  $\mathcal{G}$  by  $F(\mathcal{G}) = F(\mathcal{G}^{(0)})$ . Figure 5(a), (b), and (c) show three subgraphs whose edge weight values are less than or equal to 0.2, 0.3, and 0.4, respectively. Clearly, graph filtration affects the computation of our shortest-path graph feature maps because the shortest path changes with different sets of edges.

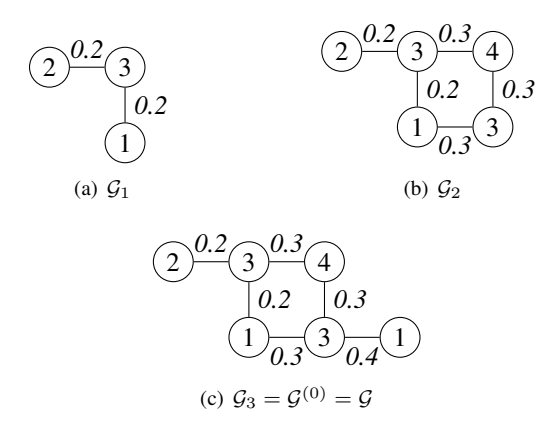


Fig. 5: The filtration of graph  $\mathcal{G}: F(\mathcal{G}) = F(\mathcal{G}^{(0)}) = \{\mathcal{G}_1, \mathcal{G}_2, \mathcal{G}_3\}$ . Numbers on edges denote edge weights.

#### D. Compute Graph Kernels

We construct a BFS tree of depth i rooted at each vertex to augment the graph vertex. The augmented graph is denoted by  $\mathcal{G}^{(i)}$ , whose graph structure is then augmented by graph filtration. For each subgraph in graph filtration, we compute the shortest-path graph feature maps and concatenate all these feature maps row-wisely as follows:

$$\Phi(\mathcal{G}^{(i)}) = \left[\phi(\mathcal{G}_1^{(i)}); \phi(\mathcal{G}_2^{(i)}); \dots; \phi(\mathcal{G}_q^{(i)})\right]$$
(6)

Finally, we have the multi-scale shortest-path filtration graph feature map as follows:

$$\Phi(\mathcal{G}) = \parallel_{i=0}^k \Phi(\mathcal{G}^{(i)}) \tag{7}$$

Following [16], we use the one-dimensional Wasserstein distance to compute the distance between the multi-scale shortest-path filtration graph feature maps of two graphs  $\mathcal{G}$  and  $\mathcal{G}'$ . The Wasserstein distance considers the distribution (frequency) of shortest paths across augmented graphs. We use the Laplacian RBF kernel to construct the multi-scale Wasserstein shortest-path filtration graph kernel (MWSPF) as follows:

$$\kappa(\mathcal{G}, \mathcal{G}') = \exp\left(-\lambda W_1(\Phi(\mathcal{G}), \Phi(\mathcal{G}'))\right) \tag{8}$$

where  $W_1(\cdot,\cdot)$  is the one-dimensional Wasserstein distance and  $\lambda$  is a hyperparameter.

#### IV. EXPERIMENTAL EVALUATION

#### A. Experimental Setup

For unweighted graphs with discrete vertex labels, we compare MWSPF with MLG [10], RetGK [4], SP [5], WL [14], DGK [24], FWL [31], and WWL [16]; for unweighted graphs with both discrete vertex labels and continuous vertex attributes, we compare MWSPF with RetGK, WWL, CSM [36], GIK [40], GH [37], HGK-SP [39] and HGK-WL [39].

We set the parameters of our MWSPF graph kernel as follows: The depth d of the BFS tree rooted at each vertex for limiting the maximum length of the shortest path is selected from  $\{0, 1, 2, ..., 6\}$ , and the depth k of the BFS tree for vertex augmentation and capturing the graph structure at multiple different scales is selected from  $\{0, 1, 2, ..., 6\}$  as well. Both d and k are selected through cross-validation on the training data. The parameters of the comparison methods are set according to their original papers. We use the implementations of MLG and WL from the GraKeL [52] library. The implementations of other graph kernels are obtained from their official websites.

We use 10-fold cross-validation with a binary C-SVM [53] (or a KSVM [50] for MWSPF and WWL) to test the classification accuracy of each method. The parameter C for each fold is independently tuned from  $\left\{10^{-3}, 10^{-2}, \ldots, 10^{3}\right\}$  using the training data from that fold. We also tune the parameter  $\lambda$  from  $\left\{10^{-4}, 10^{-3}, \ldots, 10^{1}\right\}$  for MWSPF. We repeat the experiments 10 times and report the average classification accuracy and standard deviation. In order to test the performance of our graph kernel MWSPF, we adopt 13 benchmark datasets whose statistics are given in Table I. The average shortest-path length of most datasets is lower than 6. All the datasets are downloaded from Kersting et al. [54]. We run all the experiments on a server with a dual-core Intel(R) Xeon(R) Gold 6226R CPU @ 2.90GHz, 256 GB memory, and Ubuntu 18.04.6 LTS operating system.

#### B. Results

1) Classification Accuracy: Table II demonstrates the comparison of the classification accuracy of MWSPF to other

graph kernels on the benchmark datasets with discrete vertex labels. MWSPF computes the Jaccard distance as the edge weight. MWSPF achieves the best classification accuracy on 9 out of 13 datasets. On the KKI dataset, MWSPF has a gain of 9.5% over the best comparison method FWL, which also uses graph filtration and a gain of 24.9% over the worst comparison method WWL; MWSPF is outperformed by other graph kernels on the other four datasets, i.e., COX2, PTC MR, DD, and DBLP\_v1. On the datasets COX2 and PTC\_MR, WWL achieves the best results, but the performances of MWSPF are on par with those of WWL on these two datasets. On the DD dataset, RetGK achieves the best result, but the performance gap between RetGK and MWSPF is small. On the DBLP v1 dataset, FWL is slightly better than MWSPF. DGK is a deep graph kernel that integrates neural networks in the computation of graph kernels. However, our shallow method MWSPF is superior to the deep learning graph kernel DGK on all the datasets.

Graph kernels SP and WL are the instances of the Rconvolution kernels. They do not consider the substructure distributions in graphs. Besides, SP cannot compare graphs at multiple different scales. We see that they underperform on most datasets. Compared with SP, our method MWSPF performs the best on all the datasets, which proves that our strategies to mitigate the shortcomings of SP are effective. MLG is a multi-scale graph kernel that can compute graph similarities at multiple different scales. But it also does not consider the substructure distributions in graphs. Similar to our method MWSPF, RetGK, FWL, and WWL embed each graph into the vector space and compute the similarity between two graphs by Maximum Mean Discrepancy (MMD) [21] (adopted by RetGK) or the one-dimensional Wasserstein distance (adopted by FWL, WWL, and MWSPF). However, MWSPF outperforms all of them on most datasets, which proves that the strategies of vertex augmentation and graph structure augmentation are effective.

Table III demonstrates the performances of MWSPF and comparison methods on the benchmark datasets with both discrete vertex labels and continuous vertex attributes. MWSPF computes the Euclidean distance between vertex attributes as the edge weight. We can see that MWSPF outperforms all the comparison methods on two datasets COX2 and DHFR. On the dataset PROTEINS, RetGK achieves the best result. RetGK considers each graph as a set of vertex embedding vectors, which concatenate vertex structural embedding to its continuous attributes. RetGK uses MMD to compute the distance between the two sets of vertex embeddings of two graphs. Our method MWSPF just computes the Euclidean distance between the continuous attributes of two vertices as their edge weight, based on which graph filtration is generated. Using this simple method, MWSPF is competitive with the advanced graph kernel RetGK. If we compare the same datasets in Table II and Table III, we can see that MWSPF has different results on these datasets because of the generated different graph filtrations.

2) Ablation Study: To investigate if the new shortest-path representation, vertex augmentation, graph structure augmentation, and the use of the one-dimensional Wasserstein distance

TABLE I: Statistics of the benchmark datasets used in the experiments. ASPL means the average shortest-path length of a graph while MSPL stands for the maximum shortest-path length of a graph.

Dataset	Size	Class #	Average vertex #	Average edge #	Vertex label #	ASPL	MSPL
KKI	83	2	26.96	48.42	190	4.68	19
COX2	467	2	41.22	43.45	8	6.00	18
DHFR	467	2	42.43	44.54	9	6.51	22
NCI1	4110	2	29.87	32.30	37	7.27	45
PTC_MM	336	2	13.97	14.32	20	5.34	30
PTC_MR	344	2	14.29	14.69	18	5.70	30
PTC_FM	349	2	14.11	14.48	18	5.23	30
PTC_FR	351	2	14.56	15.00	19	5.54	30
PROTEINS	1113	2	39.06	72.82	3	10.55	64
DD	1178	2	284.32	715.66	82	16.84	83
IMDB-BINARY	1000	2	19.77	96.53	N/A	1.59	2
IMDB-MULTI	1500	3	13.00	65.94	N/A	1.42	2
DBLP_v1	19456	2	10.48	19.65	N/A	2.33	4

TABLE II: The classification accuracy (mean  $\pm$  standard deviation) of MWSPF and other graph kernels on the benchmark datasets with discrete vertex labels. N/A means the results are not available owing to that GraKeL does not support that specific dataset in its current version. † means the results are adopted from the original papers.

Dataset	MWSPF	MLG	RetGK	SP	WL	DGK	FWL	WWL
KKI	56.7±5.2	48.0±3.6	48.5±3.0	50.1±3.5	50.4±2.8	51.3±4.2	51.8±11.8	45.4±12.7
COX2	$81.0\pm2.9$	$76.9 \pm 1.1$	$81.9 \pm 0.8$	80.9±1.2	81.2±1.1	78.3±0.3	$82.0\pm2.7$	$83.1 \pm 3.0$
DHFR	$85.2 \pm 4.0$	$79.6 \pm 0.5$	$82.3 \pm 0.7$	77.8±1.0	82.4±0.9	64.1±0.9	82.5±4.0	$82.7 \pm 3.6$
NCI1	86.4±1.3	80.8±1.3 <sup>†</sup>	84.5±0.2 <sup>†</sup>	73.1±0.3	82.2±0.2 <sup>†</sup>	80.3±0.5 <sup>†</sup>	85.4±1.6	85.8±0.3 <sup>†</sup>
PTC_MM	$71.4 \pm 7.0$	$61.2 \pm 1.1$	$67.9 \pm 1.4^{\dagger}$	62.2±2.2	67.2±1.6	67.1±0.5	$67.0\pm5.1$	$69.1 \pm 5.0$
PTC_MR	66.0±3.6	59.9±1.7	62.5±1.6 <sup>†</sup>	59.9±2.0	61.3±0.9	62.0±1.7	59.3±7.3	$66.3{\pm}1.2^{\dagger}$
PTC_FM	$66.2 \pm 3.7$	59.4±0.9	$63.9 \pm 1.3^{\dagger}$	61.4±1.7	$64.4\pm2.1$	64.5±0.8	$61.0\pm6.9$	65.3±6.2
PTC_FR	71.0±5.8	64.3±2.0	67.8±1.1 <sup>†</sup>	66.9±1.5	66.2±1.0	67.7±0.3	67.2±4.6	67.3±4.2
PROTEINS	77.0 $\pm$ 4.2	$76.1\pm2.0^{\dagger}$	$75.8\pm0.6^{\dagger}$	$75.8\pm0.6$	75.5±0.3	75.7±0.5 <sup>†</sup>	$74.6 \pm 3.8$	$74.3\pm0.6^{\dagger}$
DD	80.7±3.3	N/A	81.6±0.3 <sup>†</sup>	79.3±0.3	$79.8\pm0.4^{\dagger}$	73.6±0.4	78.4±2.4	79.7±0.5 <sup>†</sup>
IMDB-BINARY	$76.0 \pm 4.1$	66.2±0.8	$72.3\pm0.6^{\dagger}$	72.2±0.8	$73.8\pm3.9$	67.0±0.6 <sup>†</sup>	$72.0\pm4.6$	$73.3 \pm 4.1$
IMDB-MULTI	51.4±3.1	40.4±0.3	$48.7 \pm 0.6^{\dagger}$	50.9±0.9	50.9±3.8	44.6±0.5 <sup>†</sup>	49.5±2.6	50.4±3.5
DBLP_v1	81.8±0.8	N/A	81.8±0.1	75.5±0.5	77.6±0.6	81.2±0.5	81.9±0.8	81.8±0.6

TABLE III: The classification accuracy (mean  $\pm$  standard deviation) of MWSPF and other graph kernels on the benchmark datasets with continuous vertex attributes. N/A means the results are not available. † and ‡ indicate that the results are adopted from RetGK [4] and WWL [16], respectively.

Dataset	MWSPF	RetGK	WWL	CSM	GIK	GH	HGK-SP	HGK-WL
COX2	81.8±4.9	$81.4 \pm 0.6^{\dagger}$	78.3±0.5‡	74.4±1.7 <sup>†</sup>	N/A	$76.4\pm1.4^{\ddagger}$	72.6±1.2‡	78.1±0.5‡
DHFR	84.7±4.8	$82.5{\pm}0.8^{\dagger}$	N/A	79.9±1.1 <sup>†</sup>	N/A	N/A	N/A	N/A
PROTEINS	75.6±4.1	$78.0 {\pm} 0.3^{\dagger}$	77.9 $\pm$ 0.8 $^{\ddagger}$	N/A	76.1±0.3 <sup>†</sup>	$74.8\pm0.3^{\ddagger}$	75.8 $\pm$ 0.2 $^{\ddagger}$	$75.9\pm0.2^{\ddagger}$

TABLE IV: Comparison of classification accuracy (mean  $\pm$  standard deviation) of MWSPF to MWSP (MWSPF without graph filtration), WSP-Concat (concatenation of all the vertex labels along the shortest path as its representation and using the one-dimensional Wasserstein distance to compute graph kernels), SP-Concat (WSP-Concat without using the one-dimensional Wasserstein distance to compute graph kernels. Using instead the dot product between the feature maps of two graphs) and ordinary SP on the benchmark datasets with discrete vertex labels.

Dataset	MWSPF	MWSP	WSP-Concat	SP-Concat	SP
KKI	56.7±5.2	55.4±5.2	54.2±7.4	51.9±2.7	50.1±3.5
COX2	81.0±2.9	$80.8 \pm 4.2$	80.8±4.2	$80.9 \pm 0.7$	$80.9 \pm 1.2$
DHFR	85.2±4.0	$84.9 \pm 2.8$	84.1±3.7	$81.0 \pm 0.7$	$77.8 \pm 1.0$
NCI1	86.4±1.3	$86.1\pm1.3$	84.5±1.1	$79.2 \pm 0.3$	$73.1 \pm 0.3$
PTC_MM	71.4±7.0	$70.2\pm 5.4$	62.2±9.5	$66.9 \pm 1.0$	$62.2 \pm 2.2$
PTC_MR	66.0±3.6	$65.1\pm5.3$	60.5±5.0	$61.7 \pm 1.6$	$59.9 \pm 2.0$
PTC_FM	66.2±3.7	$65.3\pm3.1$	63.0±5.6	$62.3 \pm 0.9$	$61.4 \pm 1.7$
PTC_FR	71.0±5.8	$69.3 \pm 4.3$	67.0±2.8	$67.8 \pm 0.9$	$66.9 \pm 1.5$
PROTEINS	77.0±4.2	$76.3\pm3.4$	75.7±3.0	$75.2 \pm 0.4$	$75.8 \pm 0.6$
DD	80.7±3.3	$80.1\pm3.0$	80.1±3.0	$79.9 \pm 0.5$	$79.3 \pm 0.3$
IMDB-BINARY	76.0 $\pm$ 4.1	$74.8 \pm 3.7$	74.4±4.8	$72.7 \pm 0.7$	$72.2 \pm 0.8$
IMDB-MULTI	51.4±3.1	$51.0\pm2.6$	50.7±3.1	$49.7 \pm 0.6$	$50.9 \pm 0.9$
DBLP_v1	81.8±0.8	$81.8 \pm 0.8$	81.8±0.8	$81.9 {\pm} 0.8$	$75.5 \pm 0.5$

help to improve the performance, we compare MWSPF with MWSP (MWSPF without graph filtration), WSP-Concat (concatenation of all the vertex labels along the shortest path as its representation and using the one-dimensional Wasserstein distance), SP-Concat (WSP-Concat without using the onedimensional Wasserstein distance to compute graph kernels. Using instead the dot product between the feature maps of two graphs), and the ordinary SP on graphs with discrete vertex labels. The results are shown in Table IV. Compared with MWSP, WSP-Concat, SP-Concat, and SP, we see that MWSPF achieves the best results on 12 out of 13 datasets, which proves that our strategies of shortest-path representation, vertex augmentation, the graph structure augmentation, and the use of the one-dimensional Wasserstein distance are effective. On the dataset DBLP v1, SP-Concat has the best performance. MWSP outperforms WSP-Concat on 10 out of 13 datasets. On the remaining three datasets, MWSP and WSP-Concat perform equally well. This demonstrates that using multiple different scales of the graph structure improves performance. Compared with SP-Concat, WSP-Concat achieves the best results on 8 out of 13 datasets, which indicates the effectiveness of the use of the one-dimensional Wasserstein distance. SP-Concat outperforms SP on 10 out of 13 datasets, which proves that the new shortest-path representation is better than the triplet representation. Since we use a BFS tree of depth d (whose value is set maximally to 7) rooted at each vertex to limit the maximum length of the shortest path, this strategy may not consider all the shortest paths in a graph. Thus, SP-Concat is defeated by SP on the dataset PROTEINS.

3) Parameter Sensitivity: To analyze how the two parameters d and k affect the performance of MWSPF, we report the average classification accuracy over the 10-fold on two datasets COX2 and DHFR. These two datasets have both discrete vertex labels and continuous vertex attributes. For each dataset, we report the results of two versions of MWSPF: the first version uses the Jaccard distance to compute edge weight and the second version uses the Euclidean distance between vertex attributes to compute edge weight. Thus, these two versions differ only in the way of generating graph filtrations. Figure 6 and Figure 7 show the results. We can see that d and k have different patterns for different datasets.

We first investigate the effect of the parameter d (k is set to zero). On the dataset COX2, the best results are achieved when  $d \leq 1$ . On the dataset DHFR, the results become better with the increasing number of d. On the dataset COX2, compared with the first version, the second version has a different shape of the curve, which indicates that different graph filtrations affect the performance of MWSPF. On the dataset DHFR, the two versions have similar shapes of curves.

Next, we investigate the effect of parameter k (d is set to zero). On the dataset COX2, both the two versions tend to descend when increasing the number of k. The performance of the second version first increases and then decreases when the number of k increases. On the dataset DHFR, the first version tends to have an increasing performance with the increasing number of k. However, as for the second version, its performance first increases and then decreases when increasing k.

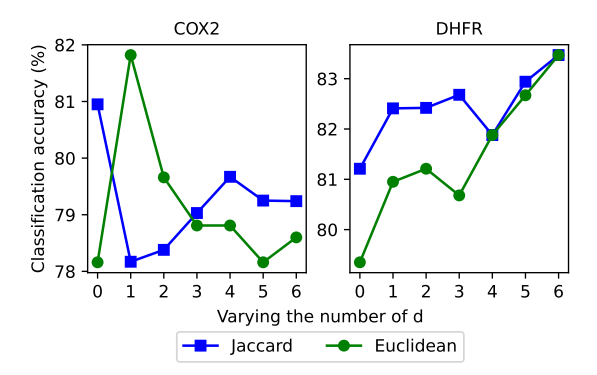


Fig. 6: Parameter sensitivity analysis on d. In legend, "Jaccard" means the version of using the Jaccard distance to compute edge weight, and "Euclidean" means the version of using the Euclidean distance between vertex attributes to compute edge weight.

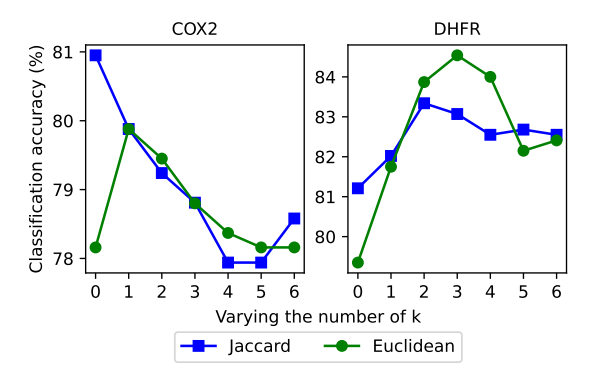


Fig. 7: Parameter sensitivity analysis on k.

#### V. CONCLUSION

In this paper, we have developed a novel multi-scale Wasserstein shortest-path filtration graph kernel called MWSPF to deal with the two challenges of the ordinary shortest-path graph kernel (SP), i.e., its triplet representation for the shortest paths may lose information and it cannot compare graphs at multiple different scales. Specifically, we construct a BFS tree of a certain depth rooted at each vertex to limit the maximum length of the shortest path to be counted considering the small world property. We concatenate all the labels of vertices in the shortest path as its representation. To make SP multi-scale, we augment not only the graph vertex but also the graph structure. The former augmentation aggregates the multiple different scales of the neighborhood graph structure into a vertex while the latter augmentation divides the graph structure into multiple different scales by graph filtrations. We use the one-dimensional Wasserstein distance to consider the changes of the frequencies of the shortest paths across the augmented graphs. Experimental results show that MWSPF outperforms other graph kernels on most graph benchmark datasets. In the future, we would like to develop a new distance measure for computing graph kernels, which can be aware of graph cluster structure information and is more efficient than the one-dimensional Wasserstein distance.

#### REFERENCES

- D. Haussler, "Convolution kernels on discrete structures," Technical report, Department of Computer Science, University of California at Santa Cruz, Tech. Rep., 1999.
- [2] T. Gärtner, P. Flach, and S. Wrobel, "On graph kernels: Hardness results and efficient alternatives," in *Learning theory and kernel machines*. Springer, 2003, pp. 129–143.
- [3] S. V. N. Vishwanathan, N. N. Schraudolph, R. Kondor, and K. M. Borgwardt, "Graph kernels," *JMLR*, vol. 11, no. Apr, pp. 1201–1242, 2010
- [4] Z. Zhang, M. Wang, Y. Xiang, Y. Huang, and A. Nehorai, "Retgk: Graph kernels based on return probabilities of random walks," in *NeurIPS*, 2018, pp. 3964–3974.
- [5] K. M. Borgwardt and H.-P. Kriegel, "Shortest-path kernels on graphs," in *ICDM*. IEEE, 2005, pp. 8–pp.
- [6] W. Ye, Z. Wang, R. Redberg, and A. Singh, "Tree++: Truncated tree based graph kernels," *IEEE TKDE*, 2019.
- [7] N. Shervashidze, S. Vishwanathan, T. Petri, K. Mehlhorn, and K. Borgwardt, "Efficient graphlet kernels for large graph comparison," in AIS-TATS, 2009, pp. 488–495.
- [8] F. Costa and K. D. Grave, "Fast neighborhood subgraph pairwise distance kernel," in ICML. Omnipress, 2010, pp. 255–262.
- [9] T. Horváth, T. Gärtner, and S. Wrobel, "Cyclic pattern kernels for predictive graph mining," in SIGKDD. ACM, 2004, pp. 158–167.
- [10] R. Kondor and H. Pan, "The multiscale laplacian graph kernel," in NeurIPS, 2016, pp. 2990–2998.
- [11] J. Ramon and T. Gärtner, "Expressivity versus efficiency of graph kernels," in *Proceedings of the first international workshop on mining graphs, trees and sequences*, 2003, pp. 65–74.
- [12] P. Mahé and J.-P. Vert, "Graph kernels based on tree patterns for molecules," *Machine learning*, vol. 75, no. 1, pp. 3–35, 2009.
- [13] N. Shervashidze and K. M. Borgwardt, "Fast subtree kernels on graphs," in *NeurIPS*, 2009, pp. 1660–1668.
- [14] N. Shervashidze, P. Schweitzer, E. J. v. Leeuwen, K. Mehlhorn, and K. M. Borgwardt, "Weisfeiler-lehman graph kernels," *JMLR*, vol. 12, no. Sep, pp. 2539–2561, 2011.
- [15] G. Da San Martino, N. Navarin, and A. Sperduti, "A tree-based kernel for graphs," in SDM. SIAM, 2012, pp. 975–986.
- [16] M. Togninalli, E. Ghisu, F. Llinares-López, B. A. Rieck, and K. Borg-wardt, "Wasserstein weisfeiler-lehman graph kernels," *NeurIPS*, vol. 9, pp. 6407–6417, 2020.
- [17] D. J. Watts and S. H. Strogatz, "Collective dynamics of 'small-world' networks," nature, vol. 393, no. 6684, pp. 440–442, 1998.
- [18] F. Harary, "Graph theory addison-wesley reading ma usa," 1969.
- [19] R. Andersen, F. Chung, and K. Lang, "Local graph partitioning using pagerank vectors," in FOCS. IEEE, 2006, pp. 475–486.
- [20] F. Chung, "The heat kernel as the pagerank of a graph," PNAS, vol. 104, no. 50, pp. 19735–19740, 2007.
- [21] A. Gretton, K. M. Borgwardt, M. J. Rasch, B. Schölkopf, and A. Smola, "A kernel two-sample test," *JMLR*, vol. 13, no. 1, pp. 723–773, 2012.
- [22] B. Weisfeiler and A. Lehman, "A reduction of a graph to a canonical form and an algebra arising during this reduction," *Nauchno-Technicheskaya Informatsia*, vol. 2, no. 9, pp. 12–16, 1968.
- [23] T. N. Kipf and M. Welling, "Semi-supervised classification with graph convolutional networks," *ICLR*, 2016.
- [24] P. Yanardag and S. Vishwanathan, "Deep graph kernels," in SIGKDD. ACM, 2015, pp. 1365–1374.
- [25] T. Mikolov, K. Chen, G. Corrado, and J. Dean, "Efficient estimation of word representations in vector space," arXiv preprint arXiv:1301.3781, 2013.
- [26] N. M. Kriege, P.-L. Giscard, and R. Wilson, "On valid optimal assignment kernels and applications to graph classification," in *NeurIPS*, 2016, pp. 1623–1631.
- [27] G. Nikolentzos, P. Meladianos, and M. Vazirgiannis, "Matching node embeddings for graph similarity," in AAAI, 2017.
- [28] S. Lazebnik, C. Schmid, and J. Ponce, "Beyond bags of features: Spatial pyramid matching for recognizing natural scene categories," in CVPR, vol. 2. IEEE, 2006, pp. 2169–2178.
- [29] K. Grauman and T. Darrell, "The pyramid match kernel: Efficient learning with sets of features." JMLR, vol. 8, no. 4, 2007.
- [30] L. Bai, L. Cui, and H. Edwin, "A hierarchical transitive-aligned graph kernel for un-attributed graphs," in *International Conference on Machine Learning*. PMLR, 2022, pp. 1327–1336.
- [31] T. H. Schulz, P. Welke, and S. Wrobel, "Graph filtration kernels," in AAAI, 2022.

- [32] S. S. Du, K. Hou, B. Póczos, R. Salakhutdinov, R. Wang, and K. Xu, "Graph neural tangent kernel: Fusing graph neural networks with graph kernels." in *NeurIPS*, 2019.
- [33] A. Jacot, F. Gabriel, and C. Hongler, "Neural tangent kernel: Convergence and generalization in neural networks," in *NeurIPS*, 2018, pp. 8571–8580.
- [34] S. Arora, S. S. Du, W. Hu, Z. Li, R. Salakhutdinov, and R. Wang, "On exact computation with an infinitely wide neural net," arXiv preprint arXiv:1904.11955, 2019.
- [35] Y. Tang and J. Yan, "Graphqntk: Quantum neural tangent kernel for graph data," in NeurIPS, 2022.
- [36] N. Kriege and P. Mutzel, "Subgraph matching kernels for attributed graphs," arXiv preprint arXiv:1206.6483, 2012.
- [37] A. Feragen, N. Kasenburg, J. Petersen, M. de Bruijne, and K. Borgwardt, "Scalable kernels for graphs with continuous attributes," in *NeurIPS*, 2013, pp. 216–224.
- [38] G. Da San Martino, N. Navarin, and A. Sperduti, "Tree-based kernel for graphs with continuous attributes," *IEEE TNNLS*, vol. 29, no. 7, pp. 3270–3276, 2017.
- [39] C. Morris, N. M. Kriege, K. Kersting, and P. Mutzel, "Faster kernels for graphs with continuous attributes via hashing," in *ICDM*. IEEE, 2016, pp. 1095–1100.
- [40] F. Orsini, P. Frasconi, and L. De Raedt, "Graph invariant kernels," in *IJCAI*, 2015, pp. 3756–3762.
- [41] B.-C. Xu, K. M. Ting, and Y. Jiang, "Isolation graph kernel," in AAAI, vol. 35, no. 12, 2021, pp. 10487–10495.
- [42] K. M. Ting, Y. Zhu, and Z.-H. Zhou, "Isolation kernel and its effect on svm," in SIGKDD, 2018, pp. 2329–2337.
- [43] K. Muandet, K. Fukumizu, B. Sriperumbudur, B. Schölkopf et al., "Kernel mean embedding of distributions: A review and beyond," Foundations and Trends® in Machine Learning, vol. 10, no. 1-2, pp. 1–141, 2017.
- [44] Y. Rubner, C. Tomasi, and L. J. Guibas, "The earth mover's distance as a metric for image retrieval," *International journal of computer vision*, vol. 40, no. 2, pp. 99–121, 2000.
- [45] H. Edelsbrunner, D. Letscher, and A. Zomorodian, "Topological persistence and simplification," in *Proceedings 41st annual symposium on foundations of computer science*. IEEE, 2000, pp. 454–463.
- [46] L. O'Bray, B. Rieck, and K. Borgwardt, "Filtration curves for graph representation," in SIGKDD, 2021, pp. 1267–1275.
- [47] G. Peyré, M. Cuturi et al., "Computational optimal transport: With applications to data science," Foundations and Trends® in Machine Learning, vol. 11, no. 5-6, pp. 355–607, 2019.
- [48] A. Figalli and C. Villani, "Optimal transport and curvature," in *Nonlinear PDE's and Applications*. Springer, 2011, pp. 171–217.
- [49] B. Haasdonk and C. Bahlmann, "Learning with distance substitution kernels," in *Joint pattern recognition symposium*. Springer, 2004, pp. 220–227.
- [50] G. Loosli, S. Canu, and C. S. Ong, "Learning svm in kreĭn spaces," IEEE TPAMI, vol. 38, no. 6, pp. 1204–1216, 2015.
- [51] M. Togninalli, E. Ghisu, F. Llinares-López, B. Rieck, and K. Borgwardt, "Wasserstein weisfeiler-lehman graph kernels," *NeurIPS*, vol. 32, 2019.
- [52] G. Siglidis, G. Nikolentzos, S. Limnios, C. Giatsidis, K. Skianis, and M. Vazirgiannis, "Grakel: A graph kernel library in python," arXiv preprint arXiv:1806.02193, 2018.
- [53] C.-C. Chang and C.-J. Lin, "Libsvm: a library for support vector machines," TIST, vol. 2, no. 3, p. 27, 2011.
- [54] K. Kersting, N. M. Kriege, C. Morris, P. Mutzel, and M. Neumann, "Benchmark data sets for graph kernels," 2016. [Online]. Available: http://graphkernels.cs.tu-dortmund.de
- [55] S. Pan, J. Wu, X. Zhu, G. Long, and C. Zhang, "Task sensitive feature exploration and learning for multitask graph classification," *IEEE transactions on cybernetics*, vol. 47, no. 3, pp. 744–758, 2017.
- [56] J. J. Sutherland, L. A. O'brien, and D. F. Weaver, "Spline-fitting with a genetic algorithm: A method for developing classification structureactivity relationships," *Journal of chemical information and computer* sciences, vol. 43, no. 6, pp. 1906–1915, 2003.
- [57] N. Wale, I. A. Watson, and G. Karypis, "Comparison of descriptor spaces for chemical compound retrieval and classification," *Knowledge and Information Systems*, vol. 14, no. 3, pp. 347–375, 2008.
- [58] K. M. Borgwardt, C. S. Ong, S. Schönauer, S. Vishwanathan, A. J. Smola, and H.-P. Kriegel, "Protein function prediction via graph kernels," *Bioinformatics*, vol. 21, no. suppl\_1, pp. i47–i56, 2005.
- [59] P. D. Dobson and A. J. Doig, "Distinguishing enzyme structures from non-enzymes without alignments," *Journal of molecular biology*, vol. 330, no. 4, pp. 771–783, 2003.

[60] S. Pan, X. Zhu, C. Zhang, and S. Y. Philip, "Graph stream classification using labeled and unlabeled graphs," in 2013 IEEE 29th International Conference on Data Engineering (ICDE). IEEE, 2013, pp. 398–409.